Synthesis of Candidate Advanced Technology Fuel: Uranium Diboride (UB2) via Carbo/Borothermic Reduction of UO2

Turner, Joel; Martini, Fabio; Buckley, James; Phillips, G; Middleburgh, Simon; Abram, Tim

Journal of Nuclear Materials

DOI:
https://doi.org/10.1016/j.jnucmat.2020.152388

Published: 01/11/2020

Peer reviewed version

7

Synthesis of Candidate Advanced Technology Fuel: Uranium Diboride (UB_2) via Carbo/Borothermic Reduction of UO_2

J. Turner[1], F. Martini[2], J. Buckley[1], G. Phillips[1], S.C. Middleburgh[2], T.J. Abram[1]

[1]*Nuclear Fuel Centre of Excellence, The University of Manchester, United Kingdom*

[2]*Nuclear Futures Institute, Bangor University, Bangor, LL57 1UT, United Kingdom*

Abstract

The synthesis of uranium diboride (UB_2) from uranium dioxide (UO_2) has been carried out for the first time after a coordinated experimental and theoretical investigation. The reliable conversion of UO_2 to UB_2 is of importance when considering commercially relevant products (e.g. as an advanced technology fuel - ATF), avoiding the use of uranium metal as a reactant. UO_2 was reduced and borated in-situ through careful combination with boron carbide (B_4C) and graphite (carbo/borothermic reduction). The reaction is observed to only be favourable at low partial pressures of CO, here made possible through use of a vacuum furnace at temperatures up to 1800 °C. At higher partial pressures of CO, the product of the reaction is UB_4. For phase pure UB_2, excess B_4C is required due to the formation of volatile boron oxides that are released from the reaction mixture as is observed when synthesising other borides through similar routes.

Keywords: Nuclear, Fuel, Uranium, High Density Fuels

1. Introduction

Uranium diboride (UB_2) is a refractory ceramic with physical properties that make it a promising candidate for the development of high-performance nuclear materials, including fuel. UB_2 has a higher uranium density compared to uranium dioxide (11.68 g cm^{-3} and 9.67 g cm^{-3}, respectively [1]), similar to other accident tolerant fuels/advanced technology candidate fuels (ATFs) such as U_3Si_2 (11.31 g cm^{-3} [2]). UB_2 also has a much higher thermal conductivity compared to UO_2 [3, 4], which will result in a lower fuel centre-line temperatures during normal operating conditions and a significantly flatter temperature profile across the pellet. This has a number of beneficial effects: (1) reducing the rate of the temperature-dependent release of fission products, (2) reduction in the pellet strain as a result of thermal expansion (which is similar to that of UO_2), (3) a reduction in the amount of thermal energy stored inside the fuel and importantly (4) a significant increase in the margin to centre-line melting.

At the same time, a higher spatial density of uranium allows more fissile material to be loaded for a given core layout - thereby extending the interval between refuelling outages and improving the fuel-cycle economics. Similarly, UB_2 can be used as a burnable absorber material further improving the fissile content within a core, extending residence times and again improving fuel-cycle economics.

Borides have historically not been explored as fuel materials, due to the high neutron absorption cross section of boron-10, which comprises approximately 20 at.% of boron found naturally. The enrichment of boron to increase boron-10 content for use in nuclear control systems is well established, while relatively isotopically pure boron-11 is used in a number of electronic components that require stability in a radiation environment [5]. There therefore exist industrial-scale methods for isotopic enrichment of elemental boron, albeit potentially not at the scale required for fuel manufacture at present.

A key challenge to developing an alternative to UO_2 is that of synthesis and fabrication. UO_2 has a number of economical and scalable synthesis routes (including the integrated dry route [6] and wet routes, for example the AUC process [7]) converting uranium hexafluoride (UF_6) to UO_2. Difficulty identifying a route for conversion either from fluoride or from oxide starting materials (widely available and relatively easy to handle) has dampened the enthusiasm for other ATF candidate fuels, including U_3Si_2.

Presently, the only reported route for UB_2 preparation is by melting elemental uranium and boron in stoichiometric amounts [3, 8, 9, 10, 32]. This procedure is only suitable for the preparation of small quantities of uranium diboride in a laboratory setting, (uranium powder is pyrophoric and not economical to produce). It must also be noted that the precipitation of uranium diboride from melts of uranium and boron affords products with significant compositional inhomogeneity [3] that would require multiple cycles of solidification, crushing and remelting to achieve a consistent stoichiometry throughout the sample. UB_4 was also produced by fused-salt electrolysis methods, for example in studies by Andrieux [36].

The development of an alternative, safer and more reliable route could allow larger amounts of UB_2 to be available for testing and evaluation. In particular, it would be highly desirable to use uranium dioxide as a precursor owing to the wealth of industrial experience and well-established techniques regarding its preparation and handling. Past work has used B_2O_3 or B_4C with an oxide that is then reduced at elevated temperatures forming the desired boride phase [37, 38, 39, 40, 41].

The purpose of the present work is therefore to demonstrate that UB_2 may be synthesised through a carbo/borothermic route from a UO_2 precursor, avoiding the need for uranium metal fabrication and/or high temperature melting. It consists of a theoretical thermodynamics study on the required conditions and reactions for UB_2 formation, and experimental demonstration of UB_2 synthesis through the theoretical route.

2. Theory

The concept of carbo/borothermic reduction has long been applied in the industrial synthesis of diboride ceramics such as zirconium diboride (ZrB_2) [11], which is isostructural with UB_2 and has a similar chemistry [12].

$$2ZrO_{2(s)} + B_4C_{(s)} + 3C_{(s)} \longrightarrow 2ZrB_{2(s)} + 4CO_{(g)} \quad (1)$$

By analogy, the borocarbothermal route may be extended to the preparation of UB_2.

$$2UO_{2(s)} + B_4C_{(s)} + 3C_{(s)} \longrightarrow 2UB_{2(s)} + 4CO_{(g)} \quad (2)$$

An excess of boron is typically required in the starting material of this route, due to the presence of relatively volatile boron species in the reaction system [13]. The active removal of carbon monoxide can be used to make reaction 2 more favourable.

A thermodynamic evaluation of the reactions was carried out to determine the conditions under which they may occur. In its most general form, the Gibbs free energy depends on temperature and pressure. In the present case the effect of pressure on the condensed phases was assumed to be negligible and the pressure sensitivity was wholly ascribed to gaseous CO, allowing us to write:

$$\Delta G_{RXN}(p_{CO}, T) = \Delta H^{\ominus}_{RXN}(T) - T \cdot \Delta S^{\ominus}_{RXN}(T) + C_{CO} \cdot RT \cdot \ln(\frac{p_{CO}}{p^{\ominus}}) \quad (3)$$

Where $\Delta G_{RXN}(p_{CO}, T)$ is the variation in Gibbs free energy at a given temperature T and a given partial pressure of carbon monoxide in the headspace P_{CO}, $\Delta H^{\ominus}_{RXN}(T)$ and $\Delta S^{\ominus}_{RXN}(T)$ are respectively the standard variations in enthalpy and entropy at a given temperature, C_{CO} is the stoichiometric coefficient with which CO is featured in the reaction and $p^{\ominus}$ is the standard state pressure of 1 bar.

3. Thermodynamic Modelling

The thermodynamic properties of most of the substances involved in the reaction model described are widely reported in literature and were immediately available through the NIST database. Data for UO_2 was taken from [35] and [23] as representative data from the extensive literature on the material. Conversely, the thermodynamic properties of UB_2 and UB_4 are not readily available and as such we have used quantum mechanical calculations based on density functional theory to complement the available data for those compounds, providing a robust set of predictions relevant to the synthesis of UB_2. Table 1 summarises the available literature data on the compounds of interest.

Table 1: Available literature data on compounds of interest. Data for diboron trioxide are referred to its liquid state, since the synthesis takes place above its melting point of 723 K [20].

Substance	$\Delta_f H^{\ominus}$ **at 298 K (kJ/mol)**	$S^{\ominus}$ **at 298 K (J/mol·K)**	**Other data**
$B_2O_{3(l)}$	-1253.36 [20]	78.45 [20]	C_p(T) function [20]
$B_4C_{(s)}$	-62.68 [20]	26.77 [20]	C_p(T) function [20]
$C_{(s)}$	0.00	5.74 [35]	C_p(T) function [21]
$CO_{(g)}$	-110.53 [20]	197.66 [20]	C_p(T) function [20]
$UB_{2(s)}$	-164.85 [10]	55.1 [10]	C_p(T) function [30]
$UB_{4(s)}$	-234.18 [30], -245.60 [22]	68.41 [30] 71.13, [22]	C_p(T) function [30]
$UO_{2(s)}$	-1085.0 [35]	77.03 [35]	C_p(T) function [23]

The enthalpy and the entropy of formation of UB_2 and UB_4 as functions of temperature were estimated via density functional theory (DFT) calculations, performed with the Vienna ab-initio simulation package (VASP) [14, 15, 16] and Phonopy [17].

For the VASP calculations, the projector augmented wave (PAW) potentials [18] were used in conjunction with the generalised gradient approximation (GGA) exchange correlation functional described by Perdew, Burke and Ernzerhof [19].

VASP was used to calculate the total energy per formula unit of crystalline structures of α-U [29], B [28], UB_2 [8] and UB_4 [8] under constant pressure, allowing cell size, shape and volume to change. Subsequently, Phonopy was used to determine the heat capacity at constant pressure per formula unit for the substances of interest.

In all calculations a convergence threshold of 10^{-8} eV was set for electronic minimisation, and a threshold of 10^{-7} eV/Å was set for geometric optimisation. The cut-off energy was set to 550 eV for all calculations with a Gaussian smearing of 0.08 eV. A Γ-centred k-point mesh was automatically generated with a constant k-point density of approximately 0.03 Å for each cell. Convergence tests were carried out with respect to the cut-off energy and the k-point density until subsequent increases resulted in changes that were smaller than 1 meV/atom. A convergence test of the smearing parameter σ was carried out by increasing its value and stopping at the maximum value which resulted in a difference between the total electronic energy and the electronic free energy smaller than 1 meV/atom.

No Hubbard correction was applied to account for electron localisation in U, UB_2 and UB_4, since elemental uranium is metallic and experimental and computational data show UB_2 [24, 25] and UB_4 [25] to have no gap between the valence and the conduction band. This is consistent with the investigations of Burr et al. [1].

The static (0 K) formation enthalpy ($\Delta_f H_{i,DFT}$) is simply predicted using DFT. To calculate the enthalpy of formation at a given temperature T ($\Delta_f H_i(T)$) it is possible to use equation 4:

$$\Delta_f H_i(T) = \Delta_f H_{i,DFT} - q_r(T) + q_P(T) \tag{4}$$

Where $q_R(T)$ and $q_P(T)$ represent the heat exchanged respectively by the reactants and the products between 0 K and the temperature T, which can be calculated by integrating their heat capacities over the same range.

The literature value for the integral of the heat capacity of UB_2 in the 0-298 K range is reported by Flotow to be 8.880 ± 0.017 kJ/mol [10], while the value calculated via DFT is 8.557 kJ/mol.

The values for the molar entropies S_i(T) of UB_2 and UB_4 were calculated by exploiting the integral definition of entropy (5), with their entropy at 0 K assumed to be nil according to the Third Law of thermodynamics:

$$S_i(T) = S_i(0K) + \int_{0K}^{298K} \frac{C_{p,i}(T')}{T'} \cdot \mathrm{d}T \tag{5}$$

The calculations yield results that are very consistent with the values obtained by experiment for UB_2 and UB_4 as shown in Table 2:

Table 2: Comparison between the values of enthalpy ($\Delta_f H$) and entropy (S) for UB_2 and UB_4 calculated in this work and those reported in the literature. Values for UB_4 reported in [30] and [22] were close but different (no uncertainties of the measurement were provided) and as such they were averaged and the uncertainty was estimated as the standard deviation between the reported measurements in this study.

Compound	$\Delta_f H$ (298 K) (kJ/mol)		S (298 K) (J/mol· K)	
	This Work	Literature	This Work	Literature
UB_2	-169.6	-165 ± 17 [10]	55.8	55.1 ± 0.1 [10]
UB_4	-245.7	-240±8 [22, 30]	67.8	69.8 ± 1.4 [22, 30]

The available data on enthalpies, entropies and heat capacities were combined to predict the behaviour of the reaction system as a function of temperature and partial pressure of CO. The molar enthalpy of formation $\Delta_f H_i(T)$ and standard molar entropy $S_i^{\ominus}$(T) for a substance i at a given temperature T were calculated according to equation 6 and 7:

$$\Delta_f H_i(T) = \Delta_f H_i(298K) + \int_{298K}^{T} C_{p,i}(T') \cdot \mathrm{d}T' \tag{6}$$

$$S_i^{\ominus}(T) = S_i^{\ominus}(298K) + \int_{298K}^{T} \frac{C_{p,i}(T')}{T'} \cdot \mathrm{d}T' \tag{7}$$

Moreover, for CO at a partial pressure p_{CO} a further correction to entropy applies:

$$S_{CO}(T, p_{CO}) = S_{CO}^{\ominus}(T) - R \cdot \ln \frac{p_{CO}}{p^{\ominus}} \tag{8}$$

Where R is the universal gas constant and $p^{\ominus}$ is the standard state pressure expressed in appropriate units (e.g 1 bar).

Based on experimental data showing the predominant formation of UB_4 over UB_2 at relatively high partial pressures of CO (see subsequent sections) and on the work of Guo et al. in the preparation of UB_4 [26], calculations were performed for three relevant compositions of the reaction mixture assuming a step-wise behaviour. A mixture prepared according to the stoichiometry dictated by reaction 9 may also host reaction 10, leading to the formation of UB_4. UB_4 may react further according to reaction 11 to finally afford UB_2.

$$2UO_{2(s)} + B_4C_{(s)} + 3C_{(s)} \longrightarrow 2UB_{2(s)} + 4CO_{(g)} \tag{9}$$

$$UO_{2(s)} + B_4C_{(s)} + C_{(s)} \longrightarrow UB_{4(s)} + 2CO_{(g)} \tag{10}$$

$$UB_{4(s)} + UO_{2(s)} + 2C_{(s)} \longrightarrow 2UB_{2(s)} + 2CO_{(g)} \tag{11}$$

Reaction 10 may be further split into the two following reactions, which can be favourable in the projected conditions of the synthesis. Reaction 12 indicates a possible pathway for the formation and subsequent loss of volatile $B_2O_{3(l)}$ from the relatively non-volatile B_4C:

$$7UO_{2(s)} + 8B_4C_{(s)} \longrightarrow 7UB_{4(s)} + 2B_2O_{3(l)} + 8CO_{(g)} \tag{12}$$

$$UO_{2(s)} + 2B_2O_{3(l)} + 8C_{(s)} \longrightarrow UB_{4(s)} + 8CO_{(g)} \tag{13}$$

The calculation of the free energy of formation for the three mixtures reported in Table 3 provides trends such as those reported in Figure 1, here with a P_{CO} of 10^{-4} bar, highlighting the most thermodynamically favourable composition of the mixture as a function of temperature (transitions at 1400 K and 1600 K) - which is the one with the most negative Gibbs free energy (ΔG). Data from these plots can be compiled to provide a phase diagram such as Figure 2, which reports the most stable composition of the solid portion of the reaction mixture as a function of temperature and CO pressure. No reaction occurs in Region 1; only reaction 12 is favourable in Region 2, meaning that any B_2O_3 that forms cannot be converted into other compounds; reaction 10 is favourable in Region 3 but reaction 12 is not, meaning that UB_4 may form via pathways that do not involve B_2O_3; both reactions 12 and 13 are favourable in Region 4, allowing UB_4 to form with B_2O_3 as an intermediate product; reaction 11 is favourable in Region 5, finally converting UB_4 into UB_2. Figure 2 clearly predicted that in order to obtain UB_2 from the borocarbothermal reduction of UO_2, a region in which UB_4 may form must be initially crossed. As such, it is expected that UB_4 may persist in the final product for kinetic reasons (e.g. non-ideal mixing).

As shown by Figure 2, operating at low values of p_{CO} gives a twofold advantage, in that it lowers the temperature at which UB_2 may be obtained and reduces the temperature interval in which UB_4 formation is preferred.

Table 3: Molar ratios of the reaction mixture under the assumption that reactions 10 and 11 proceed to completion

	Initial Mixture	**Mixture after Reaction 10**	**Mixture after Reaction 11**
UO_2	2	1	0
B_4C	1	0	0
C	3	2	0
UB_4	0	1	0
CO	0	2	4
UB_2	0	0	2

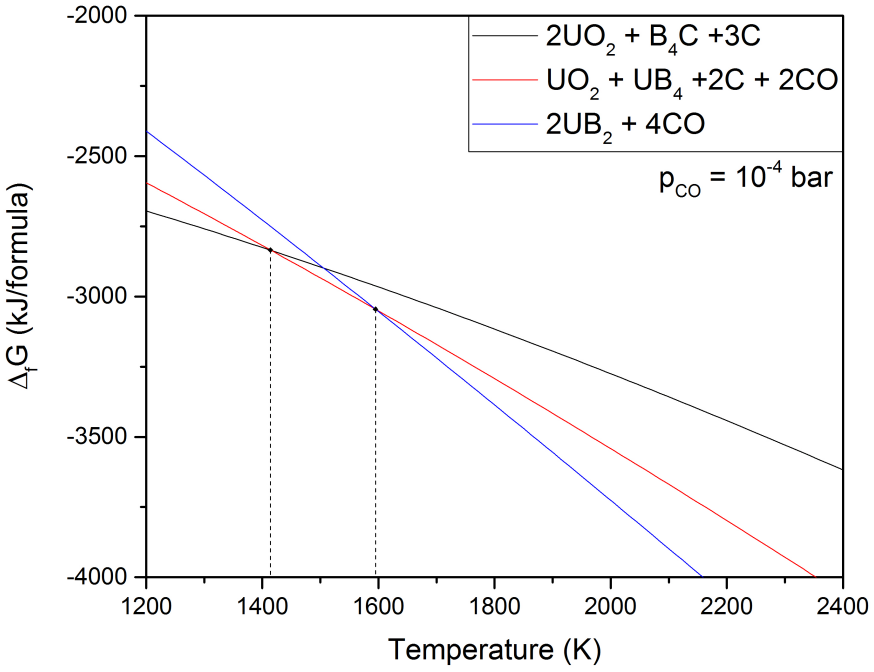

Figure 1: Free energy of formation of the three reactions considered in Table 3, calculated at a CO pressure of 10^{-4} bar

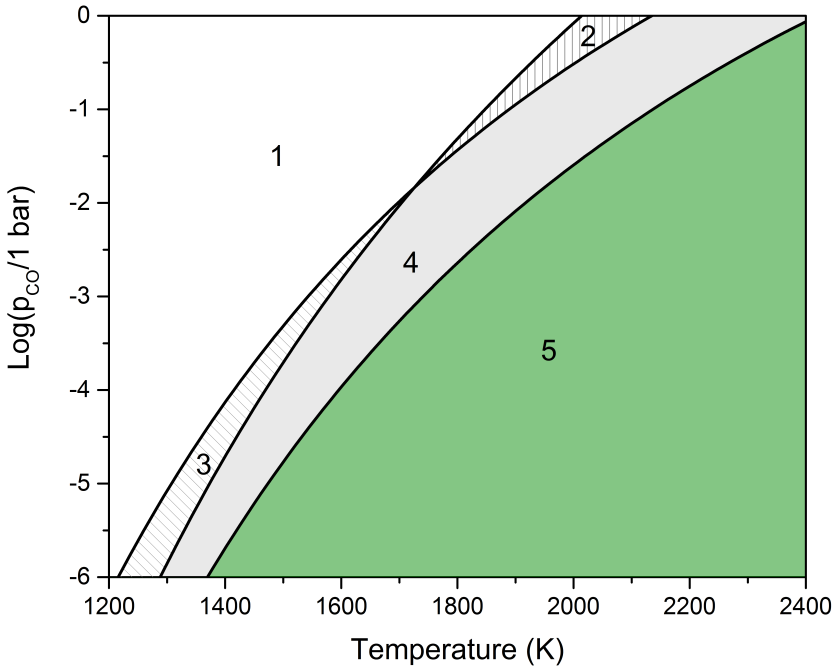

Figure 2: Phase diagram for the condensed phases of the reaction mixture for the borocarbothermal synthesis of UB_2. Region 1: UO_2, B_4C and C; Region 2: UO_2, UB_4, B_2O_3 and C; Region 3: UO_2, UB_4 and C; Region 4: UO_2, UB_4, C and B_2O_3 may form as an intermediate product; Region 5: UB_2.

4. Experimental Method

Synthesis of UB_2 from UO_2 was investigated experimentally by mixing pre-prepared powders according to reaction 2. UO_2 powder was commercially procured from ABSCO ltd (U.K.) and phase purity was confirmed via X-ray diffraction (XRD) prior to mixing, with stoichiometry measured to be 2.02±0.02 as measured using thermogravimetry. No phases other than UO_2 were detected via this method. B_4C was purchased from Sigma Aldrich (99.7% purity), while carbon powder was produced by crushing nuclear graphite (grade NBG-18). Although reaction 2 was taken as a reference, exact ratios of carbon and boron carbide were varied in an effort to improve phase purity of the final product, accounting for volatilisation of boron compounds and the production of CO_2 during lower temperature stages of the reaction, as the furnace increased in temperature.

Powders were mixed within a planetary ball mill (Retsch PBM 200) using 50 ml tungsten carbide vessels and 10 mm and/or 5 mm media at 350-400 rpm. Milling was carried out for the times listed within Table 4, with reverses of rotation every 10 minutes to ensure a well-mixed powder. Powders were mixed as a blend, carbon or boron carbide added to vary the precursor ratio and then re-milled, and so total milling times are provided within the results presented. XRD performed on blends after milling but before heat treatment did not show the formation of new phases, and it was assumed that there was insufficient energy for mechanically driven conversion.

Following milling, powders were pressed at 1 tonne/cm^2 which produced a stable and robust green pellet. Green pellets were heat treated within a graphite crucible on tantalum foil, to prevent additional carbon interaction with the material during synthesis. Initial experiments using alumina crucibles demonstrated that the material reacted with Al_2O_3 to produce a glassy phase (possibly an boro-alumina glass) which physically sealed the crucible lid in one instance.

Heat treatment was performed in a Red Devil graphite vacuum furnace (R.D. Webb Red Devil) at 1800 °C with a ramp rate of 20 °C/min and a 30 minute dwell time. All runs were started with an initial vacuum (at least 10^{-5} mbar) and operation of the turbo vacuum pump was maintained throughout. As expected, vacuum was seen to vary during operation, likely due to the release of CO during the reaction.

Material phase quantification was carried out using XRD (Malvern Panalytical Empyrian). XRD samples of synthesised material were prepared by breaking the pellet within a pestle and mortar, and grinding fragments to a fine powder before sprinkling on a silicon zero background holder. Powder was held in place using Kapton film and petroleum jelly. Phase quantification was carried out using Rietveld analysis, within the Panalyical Highscore programme.

5. Experimental Results

Initial trials were conducted in flowing Ar at 1475 °C with varied compositions and milling parameters. These tests were conducted within an STA, in an effort to observe the onset temperature of the reaction, and were not expected to produce phase pure material. However, the only phases produced with these conditions were UB_4, UC and a UBC phase first reported by Toth et al [27] and are not reported in Table 4.

Following heat treatment, mixtures appeared to form semi-sintered pellets which were solid to handle, but could easily be broken if force was applied. The colour of material post-heating varied with the phases present, as confirmed with XRD. UO_2-rich samples were dark brown or brick red in colour, while UB_2- and UB_4-rich material appeared silver or black.

Table 4: Overview of experimental trials. Molar ratio has been normalised to B_4C content. UB_2 content is rounded to ± 5% to account for relative inaccuracies within the Reitveld method, as these contents were not corroborated using an alternative method

Reference	Heat Treatment	Milling	UO_2 Molar Ratio	B_4C Molar Ratio	C Molar Ratio	UB_2 Content	Other Phases
Exp-1	1800C, vacuum	2 hours	2.10	1.00	1.01	30%	UO_2, UB_4
Exp-2	1800C, vacuum	4 hours	2.10	1.00	2.18	70%	UO_2, UB_4
Exp-3	1800C, vacuum	6 hours	2.10	1.00	3.68	85%	UO_2
Exp-4	1800C, vacuum	30 mins	2.00	1.00	2.50	0%	UB_4, C
Exp-5	1800C, vacuum	1 hour	2.00	1.00	3.00	0%	UB_4, C
Exp-6	1800C, vacuum	90 mins	2.00	1.00	3.58	90%	UC, UC_2
Exp-7	1800C, vacuum	4 hours	2.09	1.00	3.04	90%	UO_2
Exp-8	1800C, vacuum	4 hours	1.86	1.00	2.75	90%	UB_4, UO_2

Table 4 shows the phases synthesised from various heat treatments, milling durations and reactant compositions. XRD spectra of selected products are shown in Figure 3.

Synthesis performed at 1800 °Cs and under vacuum produced UB_2 apart from for Exp. 4 and 5 (although with varied phase purity). Exp. 4 and 5 were milled for comparatively short timescales, 30 and 60 mins, respectively, which may have resulted in poor mixing and therefore a lack of the desired reaction. This is supported by the presence of carbide phases within Exp-6, which do not appear in other experiments. This likely occurs from a localised excess of carbon within the mixture, and a similar mixture milled for much longer (Exp-3) contained residual UO_2, rather than carbides. Residual UO_2 is predicted for well-mixed samples as a result of volatilisation.

The material milled for four hours and containing a relative mixture of approximately $2UO_2$:B_4C:3C (Exp. 7) produced 90 % phase pure UB_2 with UO_2 as the only detectable impurity remaining.

The addition of 10 % more carbon and B_4C over that required for reaction 2 (Exp-8) produced the highest purity material, albeit it by a small margin. The UB_2 phase fraction within this material was consistently observed to be between 90 and 92% from repeated XRD analysis, while Exp 7 Experiments typically had 87-89% UB_2 from the same analysis.

6. Summary

The experimental results show that the synthesis of UB_2 from UO_2 is possible with careful consideration of the processing parameters and consideration of intermediate reactions that occur, see reaction 11. The structure of the UB_2 is $P6/mmm$ in agreement with previous investigations [3, 32] with a lattice parameter of **$a \equiv b = 3.133$ Å and $c = 3.986$ Å.**

Thermodynamic modelling performed in this study suggests that conversion of UO_2 to UB_2 will not occur unless the CO partial pressure is maintained at a sufficiently low value. Experimentally, poor CO removal was observed to result in the production of UB_4 and UBC phases in early trials in flowing argon. Similar behaviour has been reported for ZrB_2 and HfB_2 [33] and more recently for High Entropy Borides (HEBs) [13].

The conversion of the expected initial reaction product, UB_4, to UB_2 appears to be kinetically slow relative to its formation from UO_2. By ensuring the reaction products have a greater degree of intimate contact through thorough milling and mixing, there is a significant reduction in the

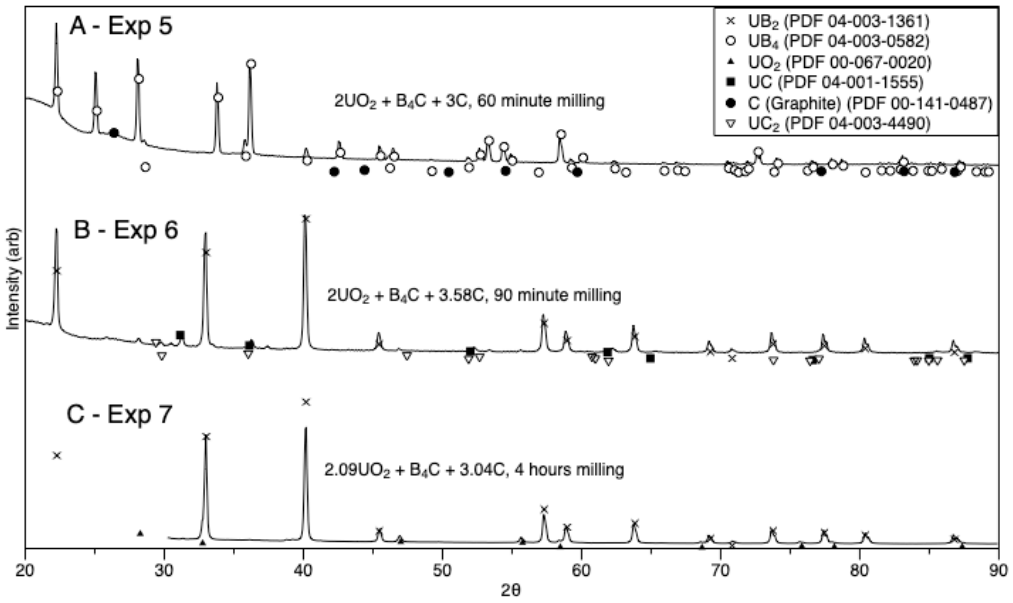

Figure 3: XRD patterns of synthesised material. A: After 60 minutes milling of stoichiometric blend, showing the formation of UB_4 only (Exp-5) B: With additional carbon and 90 minute milling, showing the production of UC alongside UB_2 (Exp-6). C: After four hours milling of stoichiometric blends, showing the synthesis of UB_2 with residual UO_2 (Exp-7). Plotted points correspond to theoretical peak positions and intensities of the reference files listed within the Figure. Data for C was only recorded down to 30 °C 2θ due to operator error.

impurity phases initially observed (mainly residual UB_4, carbon and uranium carbide formation). Further work could be considered to improve this mixing further.

Finally, the need for additional B_4C within the experiment was anticipated, due to the volatile nature of many boron compounds leading to its loss during fabrication. It is expected that UO_2 or any excess oxygen within the UO_2 will react with B_4C to produce B_2O_3, a phase that is a liquid above 450 °C with a very high vapour pressure and therefore volatility [34] (although known to enhance transport phenomena during sintering of compounds such as molybdenum silicide [31]). Any excess oxygen in the UO_2 itself will also need an appropriate amount of either C or B_4C excess to ensure full conversion is possible.

7. Data Availability

The raw/processed data required to reproduce these findings cannot be shared at this time as the data also forms part of an ongoing study

8. Acknowledgements

The authoes acknowledges the use of the Department of Materials X-ray Diffraction Suite at the University of Manchester and are grateful for the technical support, advice and assistance of Dr. John E. Warren.

Penny Dowdney, Magnus Limbck, Antoine Claisse and Mattias Puide are thanked for their support.

SCM is funded through the Sêr Cymru II programme by Welsh European Funding Office (WEFO) under the European Development Fund (ERDF). Computing resources were made available by Supercomputing Wales. FM is funded through the KESS 2 programme sponsored by Westinghouse Electric.

JB and GP are funding through the Department for Business, Energy and Industrial Strategy (BEIS) Nuclear Innovation Programme (NIP). JT is funded by the Dalton Nuclear Institute at the University of Manchester.

References

[1] P.A. Burr, E. Kardoulaki, R. Holmes, S.C. Middleburgh, J. Nucl. Mater. 513 (2019) 45-55
[2] D.A. Lopez, A. Benarosch, S. Middleburgh, K.D. Johnson, J. Nucl. Mater. 496 (2017) 234-241.
[3] E. Kardoulaki, J.T. White, D.D. Byler. D.M. Frazer, A.P. Shivprasad, T.A. Saleh, B.Gong, T.Yaob, J.Lian, K.J.McClellan, J. Alloy Comp. 818 (2020) 153216.
[4] L.J.Evitts, S.C.Middleburgh, E.Kardoulaki, I.Ipatova M.J.D.Rushton, W.E.Lee, J. Nucl. Mater. 528 (2020) 151892.
[5] R.C. Baumann, E.B. Smith, IEEE International Reliability Physics Symposium Proceedings. 38th Annual (2000).
[6] S. E. Ion R. H. Watson, 20 Years of Production of UO_2 by the Integrated Dry RouteA BNFL Perspective on Dry Conversion, A Collection of Papers on Engineering Aspects of Fabrication of Ceramics: Ceramic Engineering and Science Proceedings, Volume 14 (1993).
[7] C.S. Choi, J.H. Park, E.H. Kim, H.S. Shin, I.S. Chang, J. Nucl. Mater. 153 (1988) 148-155.
[8] J.-P. Dancausse, E. Gering, S. Heathman and U. Benedict, L. Gerward, S. Staun Olsen, F. Hulliger, J. Alloy Comp. 189 (1992) 205-208.
[9] J. Turner, T. Abram, J. Nucl. Mater. 529 (2020) 151919.
[10] H. E. Flotow, D. W. Osborne, J. Chem. Phys. 51 (1969) 583.
[11] S. Zhu, W.G. Fahrenholtz, G.E. Hilmas, S.C. Zhang, J. Am. Ceram. Soc. 90 (2007) 3660-3663.
[12] E. Jossou, D. Oladimeji, L. Malakkal, S. Middleburgh, B. Szpunar, J. Szpunara, J. Nucl. Mater. 494 (2017) 147-156.
[13] L. Feng, W.G. Fahrenholtz, G.E. Hilmas, J. Am. Ceram. Soc. 103 (2020) 724-730.
[14] G. Kresse and J. Hafner. Ab initio molecular dynamics for liquid metals. Phys. Rev. B, 47:558, 1993.

[15] G. Kresse and J. Hafner. Ab initio molecular-dynamics simulation of the liquid-metal-amorphous-semiconductor transition in germanium. Phys. Rev. B, 49:14251, 1994.
[16] G. Kresse and J. Furthmaller. Efficiency of ab-initio total energy calculations for metals and semiconductors using a plane-wave basis set. Comput. Mat. Sci., 6:15, 1996.
[17] A. Togo, I. Tanaka, Scr. Mater. 108 (2015) 1-5.
[18] P. E. Blochl. Projector augmented-wave method. Phys. Rev. B, 50:17953, 1994.
[19] J. P. Perdew, K. Burke, and M. Ernzerhof. Generalized gradient approximation made simple. Phys. Rev. Lett., 77:3865, 1996.
[20] M.W. Chase, C.A.Davies, J.R.Downey, D. Frurip, R.A.J. McDonald, Phys. Chem. Ref. Data. JANAF Thermochem. Tables 4 (1998).
[21] A.T.D. Butland, R.J. Maddison, J. Nucl. Mater. 49 (1973) 4556.
[22] I. Barin, U-WS2. Thermochemical Data of Pure Substances (1995) 17251815
[23] Y.E. Kim, J.W. Park, J. Cleveland, Thermophysical properties database of materials for light water and heavy water reactors. Int. At. Energy Agency, Vienna, Austria, Tech. Rep. IAEA-TECDOC-1496 (2006).
[24] T. Ohkochi, et al. Phys. Rev. B 78 (2008) 165110.
[25] L.L. Lohr, Int. J. Quantum Chem. 40 (1991) 121130 .
[26] H. Guo, et al. J. Am. Ceram. Soc. 102 (2019) 1049-1056.
[27] L. Toth, H. Nowotny, F. Benesovsky, E. Rudy, Monatsh. Chem. Verw. Teile. Anderer. Wiss. 92 (1961) 794802.
[28] G. Parakhonskiy, N.Dubrovinskaia, E. Bykova, R. Wirth, L. Dubrovinsky, High Press. Res. 33 (2013) 673683.
[29] A.C. Lawson, C.E. Olsen, J.W. Richardson Jnr, M. Mueller, G.H. Lander, Acta Crystallogr. Sect. B, 44 (1988) 8996 .
[30] P.Y. Chevalier, E. Fischer, Journal of Nuclear Materials, 288 (2001) 100129.
[31] J-M. Ting, Journal of Materials Science Letters, 14 (1995) 539541.
[32] L. Brewer, D.L. Sawyer, D.H. Templeton, C.H. Dauben, J. Am Ceram Soc. 34 (1951) 173-179.
[33] G-J. Zhang, W-M. Guo, D-W. Ni, Y-M. Kan, J. Phys. Conf. Ser. 176 (2008) 012041.
[34] R.H. Lamoreaux, D.L. Hildenbrand, L. Brewer, J. Phys. Chem. Ref. Data 16 (1987) 419.
[35] Medvedev, Vadim Andreevich, J. D. Cox, and Donald D. Wagman, eds. CODATA key values for thermodynamics. New York: Hemisphere Publishing Corporation, 1989.
[36] J-L Andrieux, P. Blum, "Sur La preparation electrolytique et les properietes des boures d'uranium" Compt. rend. 229 (1949) 210
[37] R. Kieffer, F, Benesovsky and E.R. Honak, Z. anorg. allg. Chem. 268 191 (1952)
[38] H.M. Greenhouse, O.E. Accountius and H.H. Sisler, J.Am. Chem. Soc. 73 5086 (1951)
[39] E. Wedekind and F. Fetzer, Ber. Dtsch. Chem. Ges. 40, 297 (1907)
[40] P. Schwarzkopf and R. Kieffer, "Refractory Hard Metals: Borides, Carbides, Nitrides, and Silicides", Macmillan, 1953
[41] N.R. Koenig, B.A. Webb "Properties of Ceramic and Cermet Fuels for Sodium Graphite Reactors" Atomics International (1960) NAASR-3880)